Inorganic Chemistry

Communication

pubs.acs.org/IC

A Luminescent Microporous Metal–Organic Framework with Highly Selective CO_2 Adsorption and Sensing of Nitro Explosives

Yun-Nan Gong, Yong-Liang Huang, Long Jiang, and Tong-Bu Lu*

MOE Key Laboratory of Bioinorganic and Synthetic Chemistry, School of Chemistry and Chemical Engineering, Sun Yat-Sen University, Guangzhou 510275, P. R. China

Supporting Information

ABSTRACT: A luminescent microporous metal–organic framework based on a π-electron-rich tricarboxylate ligand and an In^{3+} ion has been solvothermally obtained and characterized and exhibits highly selective CO_2 adsorption over CH_4 and N_2 gases and selective sensing of the nitro explosive 2,4,6-trinitrophenol.

Metal–organic frameworks (MOFs) have been extensively researched during the past decade for their structural diversity and potential applications in gas storage and separation, magnetism, catalysis, and molecular sensing.[1] Recently, MOFs have emerged as excellent sorbents for CO_2 capture and storage because of their advantages such as high surface area, tunable pore size, and low crystal density,[2] particularly for the usage of selective capture of CO_2 from natural gases.[3] Until now, only a few porous MOFs have shown highly selective adsorption of CO_2 over other gases such as CH_4 and N_2,[4] and the construction of viable CO_2-capture MOF materials that can exhibit high CO_2 selectivity over CH_4 and N_2 still remains a challenge. On the other hand, MOFs combining luminescence and permanent porosity have been of particular interest because of their potential applications as chemical sensors.[5] The rapid sensing of nitro explosives present in soil and groundwater is very crucial for security screening, homeland security, and environmental monitoring. The luminescence quenching method has proven to be a simple, sensitive, and convenient method for the sensing of such explosives.[6]

Herein, we report a luminescent microporous MOF, $(Me_2NH_2)_6[In_{10}(TTCA)_{12}]\cdot 24DMF\cdot 15H_2O$ (**1**; TTCA = triphenylene-2,6,10-tricarboxylate and DMF = *N*,*N*-dimethylformamide), that exhibits highly selective CO_2 adsorption over CH_4 and N_2 and selective sensing of the nitro explosive 2,4,6-trinitrophenol (TNP).

Solvothermal reaction of triphenylene-2,6,10-tricarboxylic acid (H_3TTCA)[7] with $In(NO_3)_3\cdot H_2O$ and hydrochloric acid in DMF and 1,4-dioxane at 170 °C for 72 h led to the formation of colorless block-shaped crystals of **1**. The result of single X-ray structural analysis reveals that **1** crystallizes in the $R\bar{3}c$ space group, which adopts a $In_3(CO_2)_8$ cluster as a secondary building unit (SBU; see Figure S1a in the Supporting Information, SI). The $In_3(CO_2)_8$ SBU contains three In atoms, which are connected by two μ_2-CO_2 and four μ_3-CO_2 groups, with an In1···In2 distance of 3.499 Å and an In1···In2···In1 angle of 167.56°. The In1 atom in the SBU is seven-coordinated with a distorted monocapped prismatic geometry, while the In2 atom is six-coordinated with a distorted octahedral geometry (Figure 1a). In **1**, each TTCA ligand links three $In_3(CO_2)_8$ SBUs to form

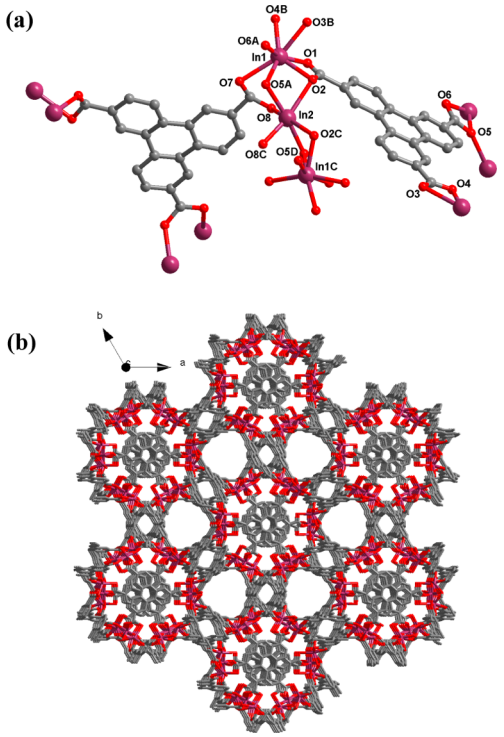

Figure 1. (a) Coordination environments of In1 and $TTCA^{3-}$ in **1** (symmetry operations: A, $-y+{}^5/_3, -x+{}^4/_3, z-{}^1/_6$; B, $-y+{}^5/_3, x-y+{}^4/_3, z+{}^1/_3$; C, $y-{}^1/_3, x+{}^1/_3, -z+{}^{11}/_6$; D, $-x+1, -y+2, -z+2$). (b) 3D microporous MOF of **1**, showing the 1D channels along the *c* axis.

a three-dimensional (3D) framework with one-dimensional (1D) channels along the *c* axis (Figure 1b); the size of the channel is 8 × 8 Å. Each $In_3(CO_2)_8$ SBU, linking eight TTCA ligands, can be regarded as an 8-connected node, and each TTCA ligand, connecting three $In_3(CO_2)_8$ SBUs, can be considered a 3-connected node, so the overall structure can be simplified to a (3,8)-connected network with $\{4^2\cdot 6\}_6\{4^3\}_2\{4^5\cdot 6^{12}\cdot 8^{10}\cdot 10^{10}\}_3$ topology (Figure S1b in the SI). Among the reported nets based on trinuclear SBUs,[8] the here-presented framework of **1** has not been observed so far.

Received: June 16, 2014
Published: August 29, 2014

dx.doi.org/10.1021/ic501413r | *Inorg. Chem.* 2014, 53, 9457–9459

The anionic framework of **1** is balanced by $Me_2NH_2^+$ cations decomposed from DMF.[9] The pores of **1** are filled with disordered $Me_2NH_2^+$, DMF, and H_2O molecules, and the solvent-accessible volume calculated using *PLATON*[10] is 48.1%. Moreover, soaking **1** in methanol leads to the exchange of DMF and H_2O molecules with methanol to give **1′**.

The results of thermogravimetric analysis (TGA) indicate that **1** readily lost DMF and H_2O molecules in the temperature range of 30−250 °C, and desolvated **1** is stable up to 350 °C, while **1′** shows plateaus from 85 to 350 °C (Figure S2 in the SI). The results of powder X-ray diffraction (PXRD) measurements of **1** and **1′** demonstrate that the framework of **1** is stable in methanol (Figure S3 in the SI). The results of variable-temperature PXRD measurements demonstrate that the framework of **1** is stable up to 270 °C (Figure S4 in the SI).

In order to evaluate the porous features of **1**, gas adsorption studies were conducted. As shown in Figure 2, N_2 adsorption

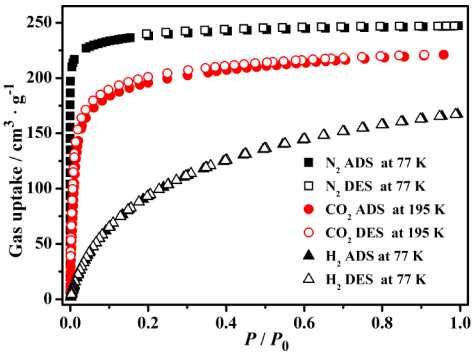

Figure 2. N_2 and H_2 adsorption isotherms of **1** at 77 K and CO_2 adsorption isotherm of **1** at 195 K.

measurement for **1** at 77 K and 1 atm revealed a reversible type I isotherm with saturated N_2 uptake of 247 cm^3 g^{-1} (STP), a characteristic of microporous materials, corresponding to a Brunauer−Emmett−Teller surface area of 726.8 m^2 g^{-1}. H_2 adsorption isotherm of **1** measured at 77 K demonstrated an uptake of 167 cm^3 g^{-1} (STP) at 1 atm. Furthermore, the adsorption isotherm of CO_2 also shows a typical type I curve, with the amounts of CO_2 uptake increasing abruptly at the beginning and then gradually reaching a plateau of 221 cm^3 g^{-1} (STP) at 195 K and 1 atm.

To further examine the gas storage capacity of **1**, we also measured the CO_2, CH_4, and N_2 sorptions at near room temperature. Interestingly, **1** shows highly selective gas adsorption for CO_2 over CH_4 and N_2 at 273 and 298 K. The CO_2 uptakes at 1 atm reach 105.2 cm^3 g^{-1} (4.69 mmol g^{-1}, 20.6 wt %) at 273 K and 69.0 cm^3 g^{-1} (3.08 mmol g^{-1}, 13.5 wt %) at 298 K. For comparison, the CH_4 and N_2 uptakes are 30.2/18.3 and 7.0/4.3 cm^3 g^{-1}, respectively, under the same conditions (Figures 3a and S5 in the SI). Using the ideal absorbed solution theory,[11] the selectivity for a 50:50 CO_2/CH_4 mixture at 273 K and 1 atm is 24 (17 at 298 K), and that for a 15:85 CO_2/N_2 mixture at 273 K and 1 atm is 221 (71 at 298 K; Figures 3b and S6 in the SI). To our knowledge, among numerous MOFs, only a few frameworks have shown the selectivities of >20 for CO_2/CH_4 and 200 for CO_2/N_2 at near room temperature.[4a−c] The highly selective adsorption of CO_2 over CH_4 and N_2 suggests that **1** may be useful for methane purification and carbon capture. The selective sorption of CO_2 rather than CH_4 and N_2 can be attributed to the quadrupole moment of CO_2 (-1.4×10^{-39}

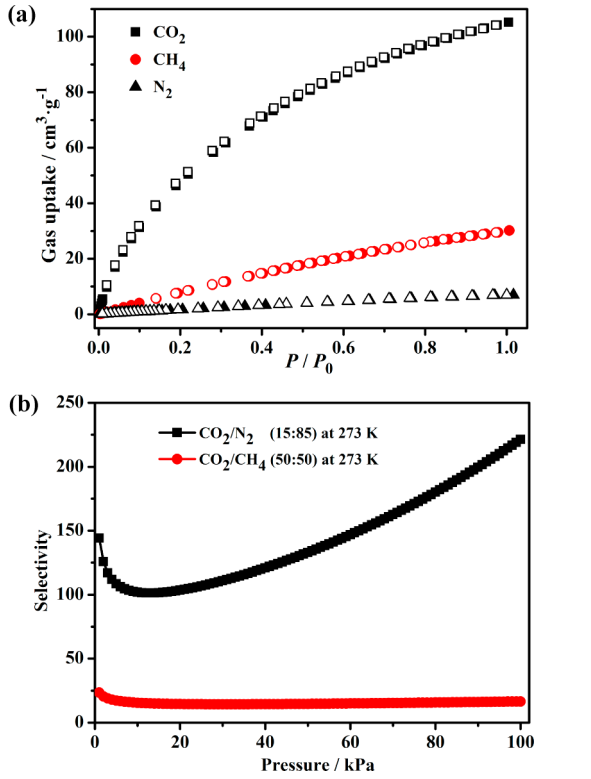

Figure 3. (a) CO_2, CH_4, and N_2 uptake curves of **1** at 273 K. (b) Adsorption selectivities of CO_2/CH_4 and CO_2/N_2 for **1** at 273 K.

cm^2), which generates specific interactions with the framework.[12] To better understand the interactions between CO_2 and the framework of **1**, we calculated the isosteric heat Q_{st} of CO_2 by fitting the 273 and 298 K isotherms to the virial equation, which is approximately 30.5 kJ mol^{-1} at zero loading (Figures S7 and S8 in the SI), implying relatively strong interactions between CO_2 and the framework of **1**.

The photoluminescence spectrum of **1** exhibits strong emission at 505 nm at ambient temperature upon excitation at 410 nm (Figure S9 in the SI), with a quantum yield of 3%, which prompts us to explore its application for the detection of electron-withdrawing compounds such as nitro explosives. Fluorescence quenching titrations were performed by adding **1** in different concentrations of methanol solutions of TNP. Figure S10 in the SI shows the quenching of luminescent intensities upon the addition of methanol solutions of TNP (0−2 mM). The maximum fluorescent intensity of **1** was reduced by 82.2% upon exposure to 2 mM methanol solutions of TNP [quenching percentage = $(I_0 - I)/I_0 \times 100\%$, where I_0 and I are fluorescent intensities of **1** before and after exposure to the nitroaromatic explosives]. Moreover, there is an obvious red shift (from 505 to 537 nm for the maximum fluorescent emission) for the spectra accompanied by quenching of the luminescent intensity upon the addition of a 2 mM methanol solution of TNP, which can be ascribed to the guest-dependent interactions between the MOF host framework and TNP (kinetic diameter ca. 7.2 Å).[6g,13] On the other hand, the luminescence responses of **1** to other nitro explosives, such as 2,4,6-trinitrotoluene (TNT), 2,4-dinitrotoluene (2,4-DNT), 2,6-dinitrotoluene (2,6-DNT), and nitrobenzene (NB), were ascertained by dispersing **1** in 2 mM nitro explosives in methanol (Figure 4). The maximum fluorescent intensity of **1** was reduced by 41.7, 62.1, 73.5, and 65.9% upon exposure to 2 mM methanol solutions of TNT, 2,4-DNT, 2,6-

dx.doi.org/10.1021/ic501413r | Inorg. Chem. 2014, 53, 9457−9459

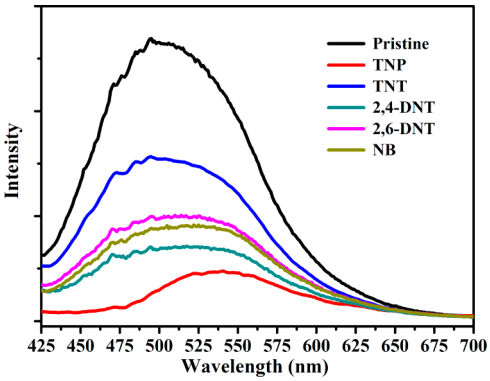

Figure 4. Luminescence changes of **1** by the addition of 2 mM methanol solutions of TNP, TNT, 2,4-DNT, 2,6-DNT, and NB.

DNT, and NB, respectively. The efficient quenching by nitro explosives can be attributed to a photoinduced electron transfer from the excited framework of **1** (as an electron donor) to the adsorbed electron acceptor (nitro explosives).[14,6e] However, unlike TNP, the maximum fluorescent emission of **1** was hardly shifted by TNT, 2,4-DNT, 2,6-DNT, and NB, indicating that **1** could be regarded as a potential material for the selective detection of the nitro explosive of TNP.

In conclusion, a 3D luminescent microporous MOF based on triphenylene-2,6,10-tricarboxylate has been constructed. The compound exhibits highly selective gas adsorption for CO_2 over CH_4 and N_2, recommending the possible applications in purification of natural gas by CO_2/CH_4 separation and capturing CO_2 from flue gases. Furthermore, it also shows selective sensing of the nitro explosive TNP, making it a promising sensing material for TNP monitoring.

■ ASSOCIATED CONTENT

Ⓢ Supporting Information

Synthesis and characterization, gas sorption measurements, additional structure figures, adsorption isotherms, adsorption selectivity and luminescenct profiles, isosteric heat isotherms, TGA, PXRD, and X-ray crystallographic data in CIF format. This material is available free of charge via the Internet at http://pubs.acs.org.

■ AUTHOR INFORMATION

Corresponding Author

*E-mail: lutongbu@mail.sysu.edu.cn.

Notes

The authors declare no competing financial interest.

■ ACKNOWLEDGMENTS

This work was financially supported by the 973 Program of China (Grants 2012CB821705 and 2014CB845602), NSFC (Grants 21331007 and 21121061), and NSF of Guangdong Province (Grant S2012030006240).

■ REFERENCES

(1) (a) Yun, R. R.; Lu, Z. Y.; Pan, Y.; You, X. Z.; Bai, J. F. *Angew. Chem., Int. Ed.* **2013**, *52*, 11282−11285. (b) Zhong, D. C.; Lu, T. B. *Sci. China Chem.* **2011**, *54*, 1395−1406. (c) Feng, D. W.; Gu, Z. Y.; Li, J. R.; Jiang, H. L.; Wei, Z. W.; Zhou, H. C. *Angew. Chem., Int. Ed.* **2012**, *51*, 10307−10310. (d) Wanderley, M. M.; Wang, C.; Wu, C. D.; Lin, W. B. *J. Am. Chem. Soc.* **2012**, *134*, 9050−9053. (e) Falkowski, J. M.; Wang, C.; Liu, S.; Lin, W. B. *Angew. Chem., Int. Ed.* **2011**, *50*, 8674−8678. (f) Liu, T. F.; Chen, Y. P.; Yakovenko, A. A.; Zhou, H. C. *J. Am. Chem. Soc.* **2012**, *134*, 17358−17361.

(2) (a) Henke, S.; Fischer, R. A. *J. Am. Chem. Soc.* **2011**, *133*, 2064−2067. (b) Sumida, K.; Rogow, D. L.; Mason, J. A.; McDonald, T. M.; Bloch, E. D.; Herm, Z. R.; Bae, T. H.; Long, J. R. *Chem. Rev.* **2012**, *112*, 724−781. (c) Xue, D. X.; Cairns, A. J.; Belmabkhout, Y.; Wojtas, L.; Liu, Y. L.; Alkordi, M. H.; Eddaoudi, M. *J. Am. Chem. Soc.* **2013**, *135*, 7660−7667.

(3) (a) Bae, Y. S.; Snurr, R. Q. *Angew. Chem., Int. Ed.* **2011**, *50*, 11586−11596. (b) Du, L. T.; Lu, Z. Y.; Zheng, K. Y.; Wang, J. Y.; Zheng, X.; Pan, Y.; You, X. Z.; Bai, J. F. *J. Am. Chem. Soc.* **2013**, *135*, 562−565.

(4) (a) Nugent, P.; Belmabkhout, Y.; Burd, S. D.; Cairns, A. J.; Luebke, R.; Forrest, K.; Pham, T.; Ma, S. Q.; Space, B.; Wojtas, L.; Eddaoudi, M.; Zaworotko, M. J. *Nature* **2013**, *495*, 80−84. (b) Xiang, S. C.; He, Y. B.; Zhang, Z. J.; Wu, H.; Zhou, W.; Krishna, R.; Chen, B. L. *Nat. Commun.* **2012**, *3*, 954−962. (c) Nugent, P. S.; Rhodus, V. L.; Pham, T.; Forrest, K.; Wojtas, L.; Space, B.; Zaworotko, M. J. *J. Am. Chem. Soc.* **2013**, *135*, 10950−10953. (d) Lu, W. G.; Sculley, J. P.; Yuan, D. Q.; Krishna, R.; Wei, Z. W.; Zhou, H. C. *Angew. Chem., Int. Ed.* **2012**, *51*, 7480−7484. (e) Bloch, W. M.; Babarao, R.; Hill, M. R.; Doonan, C. J.; Sumby, C. J. *J. Am. Chem. Soc.* **2013**, *135*, 10441−10448. (f) McDonald, T. M.; D'Alessandro, D. M.; Krishna, R.; Long, J. R. *Chem. Sci.* **2011**, *2*, 2022−2028.

(5) (a) Harbuzaru, B. V.; Corma, A.; Rey, F.; Jordá, J. L.; Ananias, D.; Carlos, L. D.; Rocha, J. *Angew. Chem., Int. Ed.* **2009**, *48*, 6476−6479. (b) Li, Y.; Zhang, S. S.; Song, D. T. *Angew. Chem., Int. Ed.* **2013**, *52*, 710−713.

(6) (a) Lan, A. J.; Li, K. H.; Wu, H. H.; Olson, D. H.; Emge, T. J.; Ki, W.; Hong, M. C.; Li, J. *Angew. Chem., Int. Ed.* **2009**, *48*, 2334−2338. (b) Gole, B.; Bar, A. K.; Mukherjee, P. S. *Chem. Commun.* **2011**, *47*, 12137−12139. (c) Pramanik, S.; Zheng, C.; Zhang, X.; Emge, T. J.; Li, J. *J. Am. Chem. Soc.* **2011**, *133*, 4153−4155. (d) Peng, Y.; Zhang, A. J.; Dong, M.; Wang, Y. W. *Chem. Commun.* **2011**, *47*, 4505−4507. (e) Gong, Y. N.; Jiang, L.; Lu, T. B. *Chem. Commun.* **2013**, *49*, 11113−11115. (f) Nagarkar, S. S.; Joarder, B.; Chaudhari, A. K.; Mukherjee, S.; Ghosh, S. K. *Angew. Chem., Int. Ed.* **2013**, *52*, 2881−2885. (g) Xue, Y. S.; He, Y. B.; Zhou, L.; Chen, F. J.; Xu, Y.; Du, H. B.; You, X. Z.; Chen, B. L. *J. Mater. Chem. A* **2013**, *1*, 4525−4530.

(7) Gong, Y. N.; Meng, M.; Zhong, D. C.; Huang, Y. L.; Jiang, L.; Lu, T. B. *Chem. Commun.* **2012**, *48*, 12002−12004.

(8) (a) Yang, E. C.; Liu, Z. Y.; Wang, X. G.; Batten, S. R.; Zhao, X. J. *CrystEngComm* **2008**, *10*, 1140−1143. (b) Gong, Y. N.; Lu, T. B. *Chem. Commun.* **2013**, *49*, 7711−7713.

(9) (a) An, J.; Rosi, N. L. *J. Am. Chem. Soc.* **2010**, *132*, 5578−5579. (b) Zheng, S. T.; Wu, T.; Irfanoglu, B.; Zuo, F.; Feng, P. Y.; Bu, X. H. *Angew. Chem., Int. Ed.* **2011**, *50*, 8034−8037.

(10) Spek, A. L. *PLATON 99: A Multipurpose Crystallographic Tool*; Utrecht University: Utrecht, The Netherlands, 1999.

(11) Bae, Y. S.; Mulfort, K. L.; Frost, H.; Ryan, P.; Punnathanam, S.; Broadbelt, L. J.; Hupp, J. T.; Snurr, R. Q. *Langmuir* **2008**, *24*, 8592−8598.

(12) Huang, Y. L.; Gong, Y. N.; Jiang, L.; Lu, T. B. *Chem. Commun.* **2013**, *49*, 1753−1755.

(13) Sun, L. B.; Xing, H. Z.; Xu, J.; Liang, Z. Q.; Yu, J. H.; Xu, R. R. *Dalton Trans.* **2013**, *42*, 5508−5513.

(14) Zhang, C. Y.; Che, Y. K.; Zhang, Z. X.; Yang, X. M.; Zang, L. *Chem. Commun.* **2011**, *47*, 2336−2338.